Episodic growth of normal faults as recorded by syntectonic sediments, July oil field, Suez rift, Egypt

David A. Pivnik, Mohamed Ramzy, Brad L. Steer, Jay Thorseth, Zarif El Sisi, Ihab Gaafar, John D. Garing, and Robert S. Tucker

ABSTRACT

The July oil field is a major normal-fault–bounded structural block in the Suez rift basin, Egypt. It is adjacent to a major structural transfer zone, which has controlled sediment influx to the rift basin center for the past 20 m.y. The lower to middle Miocene Upper Rudeis Formation, part of the synrift stratigraphic sequence, records deformation of the July structural block. The formation contains abrupt lateral changes in thickness and facies, which record earlier phases of fault movement and deformation in the July field area that do not conform to the present-day structural configuration.

The Upper Rudeis Formation was deposited as turbidites in a submarine-fan system sourced from the western rift shoulder. It was deposited over and around bathymetric highs created by coeval fault displacement in the July field area. By studying thickness and facies patterns, we have determined that the present-day main bounding fault to the July block consisted of a series of unlinked fault segments, which linked after Upper Rudeis deposition. A subsidiary fault west of the block exerted the most control on thickness patterns, not the present-day main bounding fault. Thus, commonly used models of deposition in active half grabens are difficult to apply at July field.

INTRODUCTION

Synrift sedimentary rocks in rift basins are attractive but challenging hydrocarbon reservoirs. They are attractive because large volumes of coarse clastic synrift sediment can be transported into the basin, creating high-quality reservoirs (e.g., Morley et al., 1990;

Manuscript received April 5, 2002; provisional acceptance July 17, 2002; revised manuscript received November 5, 2002; final acceptance February 5, 2003.

DOI:10.1306/02050301100

AUTHORS

DAVID A. PIVNIK ~ *BP/Gulf of Suez Petroleum Company, Palestine Street, New Maadi, Cairo, Egypt; pivnikda@bp.com*

Dave Pivnik holds degrees in geology from the State University of New York, Fredonia (B.S., 1985), University of Rochester (M.S., 1988), and Dartmouth College (Ph.D., 1992). He has been with BP (formerly Amoco) since 1993. His research and exploration efforts have focused on syntectonic sedimentary rocks in compressional, extensional, and strike-slip basins. He has been exploring for hydrocarbons in the Suez rift since 1997.

MOHAMED RAMZY ~ *Gulf of Suez Petroleum Company, Palestine Street, New Maadi, Cairo, Egypt; refaatmr@gupco.net*

Mohamed Ramzy holds a B.S. degree in geology from Alexandria University (1978). He has been with GUPCO, Amoco, and BP since 1981 as an exploration and development geologist. His research and exploration work has focused on the distribution, characterization, and deformation of prerift and synrift sedimentary rocks in the Suez rift.

BRAD L. STEER ~ *BP America Production Company, 501 Westlake Park Blvd., Houston, Texas; steerbl@bp.com*

Brad Steer holds degrees in geology from San Diego State University (M.S., 1979), University of Utah (B.S., 1976), and University of Northern Colorado (B.A., 1974). He has been with BP (formerly Amoco) since 1980. He has worked in numerous basins, including the Suez rift, Egypt, the Columbus basin, Trinidad, and, currently, the Arkoma basin, Oklahoma.

JAY THORSETH ~ *BP/Gulf of Suez Petroleum Company, Palestine Street, New Maadi, Cairo, Egypt; thorsejc@bp.com*

Jay Thorseth holds a B.S. degree in geophysics (1986) and an M.B.A. (1988) from the University of Utah. He has been with BP (formerly Amoco) since 1988. He has exploration and development experience in the United States, Russia, Azerbaijan, Kazakhstan, and Egypt. He has been exploring for hydrocarbons in the Suez rift since 1997 and is currently an exploration team leader.

ZARIF EL SISI ~ *Gulf of Suez Petroleum Company, Palestine Street, New Maadi, Cairo, Egypt; elsisiza@gupco.net*

Zarif El Sisi holds degrees in geology from Alexandria University (B.S., 1980) and sedimentology from Cairo University (M.S., 1998). He has worked for GUPCO and BP since 1984 as a sedimentologist and petrologist. His work focuses on diagenesis,

hydrocarbon shows, depositional environments, sequence stratigraphy, and reservoir characterization in the Suez rift, Egyptian western desert, and Nile Delta.

IHAB GAAFAR ~ *Gulf of Suez Petroleum Company, Palestine Street, New Maadi, Cairo, Egypt; gaffarix@gupco.net*

Ihab Gaafar holds a degree in geochemistry (B.Sc., 1979), from Al Azhar University. He has been with GUPCO since 1979 as a biostratigrapher and has worked extensively with the BP (formerly Amoco) biostratigraphy group. His exploration and research work has focused on establishing and utilizing biostratigraphic composite standards in the Suez rift and Nile Delta for chronostratigraphic and paleoenvironmental interpretations.

JOHN D. GARING ~ *BP Exploration, P.O. Box 196612, 900 E. Benson Boulevard, Anchorage, Alaska, 99519; garingjd@bp.com*

John Garing is currently a subsurface development team leader for BP in Anchorage, Alaska in the United States. He has worked for BP (formerly Amoco) since 1982 in Egypt and the western United States in exploration, development, and geophysical research. He received a B.S. degree in geological engineering from Princeton University in 1980 and an M.S. degree in geophysics from Stanford University in 1982.

ROBERT S. TUCKER ~ *Tobin International, Ltd., 1625 Broadway, Denver, Colorado; bob.tucker@tobin.com*

Bob Tucker holds degrees in geology from the University of California, Los Angeles (B.S.) and San Diego State University (M.S.) and a Master of Engineering degree from the University of Colorado, Denver. He worked for BP (formerly Amoco) as a development geologist in the Gulf of Suez for 5 years. He is currently a Geographic Information System software development quality-assurance engineer.

ACKNOWLEDGEMENTS

This paper is dedicated to the memory of Ken Loos, a first-class explorationist and friend. The manuscript benefited greatly from reviews by W. Wescott, E. Mancini, and M. Pranter and early reviews by Tim Marchant, John Dolson, and Rob Gawthorpe. We acknowledge the work of current and previous geoscientists at the Gulf of Suez Petroleum Company (GUPCO), which greatly enhanced our understanding of the Suez rift. We thank GUPCO and BP for the support in writing the manuscript.

Nelson et al., 1992; Gawthorpe and Hurst, 1993; Gupta et al., 1999; Young et al., 2000). They are challenging because sediment sources, transport pathways, and depositional basins are controlled by the positions of uplifted fault blocks and structural transfer zones (Lambiase and Bosworth, 1995). In areas with well or outcrop control or high-quality seismic data, facies patterns and thickness changes in synrift strata are perhaps our best tools to understand structural evolution. Sedimentary facies distribution, reservoir-unit isopach, petrographic, paleontologic, and seismic data should be used in concert to understand from where sediment entered a basin, how and when accommodation space was created during rift-related deformation, and where sediment was ultimately deposited. Understanding the tectonic (and other) controls on synorogenic sedimentation and resultant depositional geometries of synrift sedimentary rocks reduces hydrocarbon-exploration risk.

Models of rift basin stratigraphy have proven to be of great importance in understanding large-scale stratigraphic patterns related to rift evolution (e.g., Proser, 1993; Gawthorpe et al., 1994; Ravnas and Steel, 1998; Bosence, 1998). However, synrift sediment dispersal patterns and, ultimately, rift basin stratigraphy are abruptly affected by finer scale features such as spacially and temporally variable point sources, the three-dimensional (3-D) geometry of fault blocks, and the episodic nature of fault growth and motion. The present-day structural configuration of a fault block is a result of a complex history of fault segment growth, linkage, and displacement transfer and may not reflect the structural geometry during earlier stages of synrift deposition. Thus, the history of structural deformation may only be understood by examining the synrift strata deposited on and adjacent to a structural block. In this paper, we use thickness and facies variations of synorogenic sedimentary rocks to describe the structural evolution of the July oil field, which is hosted by a major fault block in the Suez rift. These rocks have produced approximately 64 million of the more than 650 million bbl of oil from the July field, underscoring the economic importance of understanding their distribution.

THE SUEZ RIFT

The Suez rift is a continental rift basin that initiated in the upper Oligocene to lower Miocene as the northwest extension of the Red Sea rift (Garfunkel and Bartov, 1977; Patton et al., 1994, Schutz, 1994; McClay et al., 1998; Bosworth and McClay, 2001) (Figure 1). The major normal faults in the basin strike northwest and form a complex series of tilted half grabens and asymmetric horsts (Figure 1). Northwest to southeast there are three distinct structural provinces in the rift. In each province, the dip direction of major normal faults is constant; however, the dip direction reverses 180° between provinces (Moustafa, 1976, 2002; Patton et al., 1994; Younes and McClay, 2002). Structurally complex transfer zones separate these provinces (e.g., Moustafa, 1995) (Figure 1).

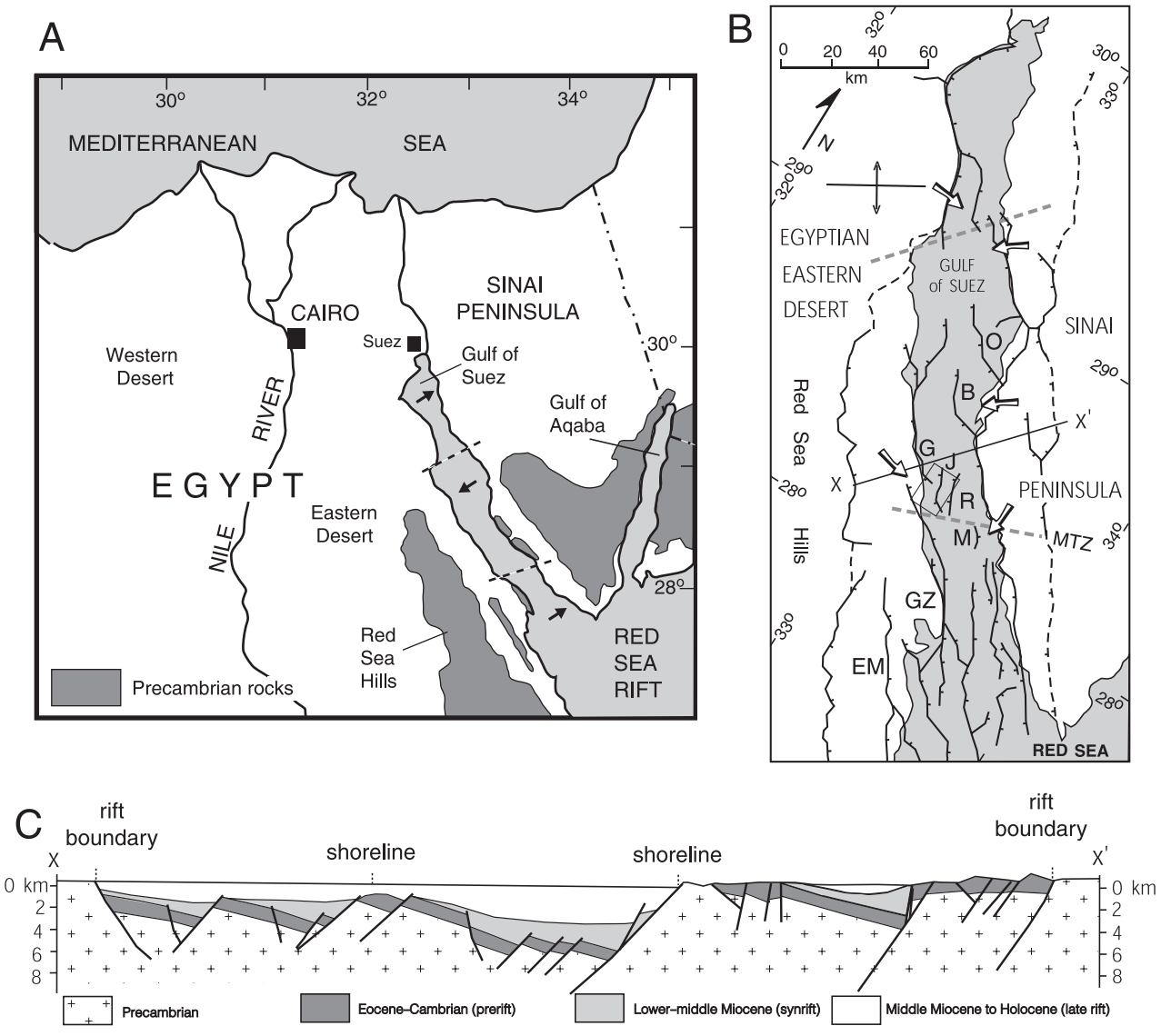

Figure 1. (A) Regional map showing northeastern Egypt, northern Red Sea rift, and Gulf of Suez. Dashed lines in the Gulf of Suez represent structural transfer zones. Black arrows represent general direction of fault dips. (B) Map of Suez rift showing major normal faults. Ticks on fault traces indicate downthrown side. Gray dashed lines are structural transfer zones. Modified from Patton et al. (1994). Highlighted arrows indicate Upper Rudeis sediment transport directions. Small box represents map area for all gross interval and net reservoir isopach maps. Abbreviations for structural high blocks and/or oil fields are as follows: B = Belayim; EM = Esh El Mallaha; G = Ras Gharib; GZ = Gebel Zeit; J = July; M = El Morgan; MTZ = Morgan transfer zone; O = October; R = Ramadan. (C) Cross section XX′, showing generally southwest-dipping normal faults and northeast-dipping bedding, common to the central region of the Suez rift. See (B) for location. Modified from Patton et al. (1994).

Miocene (and possibly Oligocene) and younger synrift deposits rest unconformably on prerift Precambrian through Eocene rocks (Figure 2). In the Suez rift, many of the largest hydrocarbon reservoirs are in Miocene synrift sedimentary rocks perched atop footwalls of normal fault blocks (e.g., Belayim land and marine fields, ~2 billion bbl; El Morgan field, ~1.5 billion bbl; July field, ~650 million bbl; Matbouly and El Sabbagh, 1996). They consist of deposits of large deltas or submarine fans originally sourced from the rift shoulders and transported to the basin via structural transfer zones (e.g., Rhine et al., 1988; El Heiny and Enani, 1990). In some cases, the reservoirs are thickest on present-day structural highs, suggesting that uplift postdated deposition of the reservoirs. Closer examination of synrift strata reveals that fault motion was episodic throughout the Miocene. Seismic-data quality in the Suez rift is poor because of multiples created by middle

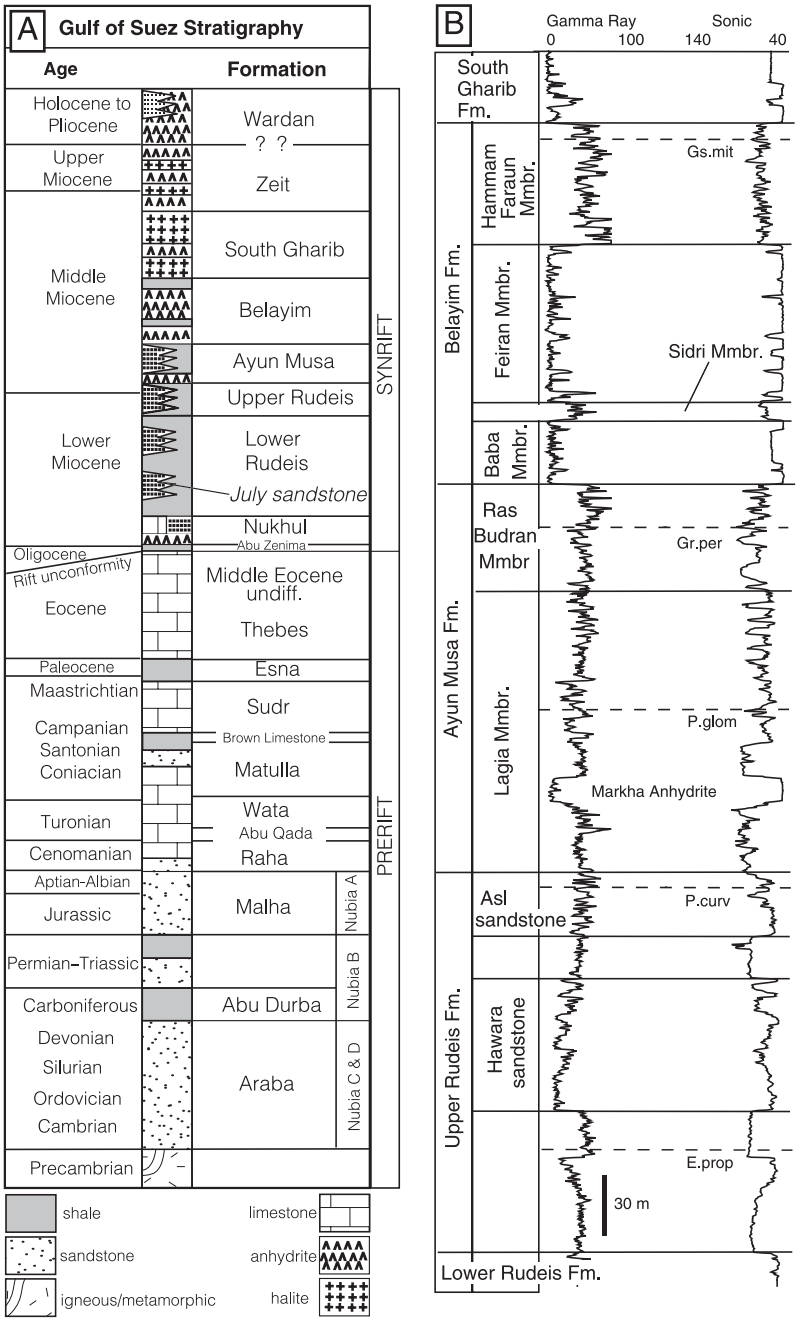

Figure 2. (A) Generalized stratigraphic column for the Suez rift. Modified from Schutz (1994). (B) Well log from J10-44 well in the west July field area. Logs are sonic (DT: 140–40 ms) and gamma ray (GR: 0–100° API). Full names for foraminiferal first appearances (abbreviated) can be found in the text. See Figure 3 for location of well.

to upper Miocene evaporites. Only by using data from abundant well control can we determine when fault segments experienced motion and linked, and how structural blocks evolved.

DATA AND METHODS

Since the middle 1960s, the Gulf of Suez Petroleum Company (GUPCO) has been the largest acreage holder and producer of hydrocarbons in the basin. As a result, GUPCO has an integrated, digital (and non-digital) database consisting of well cuttings, core, paleontologic, petrographic, and wire-line log data from approximately 2000 wells drilled both onshore and offshore, regionally extensive 3-D and 2-D seismic data, gravity and aeromagnetic data, satellite imagery, and geological data from outcrops on the rift margins and shoulders. For this study, we used data from more than 100 wells drilled in and around the July oil field, as well as 3-D seismic data and data from hundreds of additional wells from the central Suez rift to present a

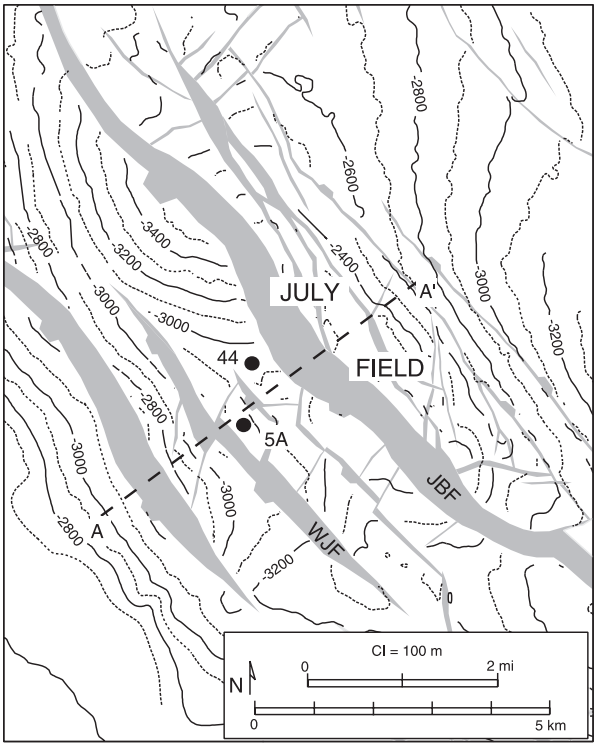

Figure 3. Structural contour map on the top of the Asl sandstone. Fault gaps at Asl level are shown in gray. WJF = west July fault; JBF = July-B fault; 5A = well SG310-5A; 44 = well J10-44. See Figure 1B for location of the map area.

well-constrained example of structural deformation controlling synrift deposition.

Correlation of formation tops in the July field area is well constrained by regionally consistent wire-line log patterns (Figure 2). We used the three available core from the Upper Rudeis Formation in the area to describe sedimentological facies and related these to the log signatures to interpret depositional environments and patterns. First downhole appearances of key foraminifera or foraminiferal assemblages occur consistently with the lithostratigraphic units and support the wire-line log correlations (Krebs et al., 1997; Wescott et al., 1996; GUPCO proprietary data) (Figure 2).

The long history of oil exploration and associated stratigraphic work in the Suez rift has resulted in an abundance of formation names in the literature and industry (National Stratigraphic Sub-Committee, 1974; Hosny et al, 1986). We use formation names partly based on the scheme proposed by Hosny et al. (1986). We focus on the Upper Rudeis Formation and lower part of the Lagia Member of the Ayun Musa Formation (Figure 2). We also refer to the Lower Rudeis, the Ayun Musa (or Kareem), and the Belayim formations.

SYNRIFT DEPOSITION AROUND JULY FIELD

July field is a large, asymmetric, generally northeast-dipping horst bounded to the southwest by southwest-dipping, large-displacement normal faults and to the northeast by northeast-dipping, smaller displacement normal faults (Figures 3, 4). The July-B fault is the major southwest-dipping, block-bounding fault and has about 1200 m (~3900 ft) of throw at the pre-Miocene level (Figure 4). A series of synthetic faults is present in the hanging wall of the July-B fault, including the west July fault, which has about 500 m (~1600 ft) of throw at the pre-Miocene level (Figure 4). Faults that strike north-northeast and northeast (cross faults) also occur in the main structural block and commonly serve as linking faults between northwest-striking, rift-parallel faults (e.g., Patton et al, 1994).

July field is located adjacent to the Morgan structural transfer zone, which separates normal faults that

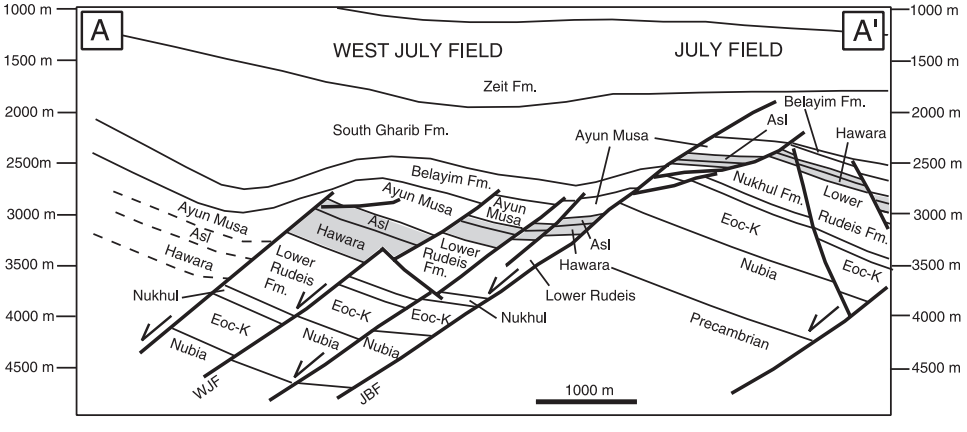

Figure 4. Structural cross section from 3-D seismic interpretation. Note dramatic thickening of Asl and Hawara units and Ayun Musa Formation on the hanging wall of the west July fault (WJF), but minimal changes across the July-B fault (JBF), which presently bounds the field. The Belayim Formation is absent on the crest of the field. See Figure 3 for location. Eoc-K = Eocene through Cretaceous.

dip to the southwest (e.g., July, Ramadan, and Ras Gharib fault blocks) and those that dip to the northeast (e.g., El Morgan, Gebel Zeit, and Gebel Esh El Malaha fault blocks; Figure 1). The Red Sea Hills expose Precambrian rocks at the surface and served as a major source for coarse-grained sediment transported into the July field area for most of the history of the Suez rift. This depositional system is still expressed by modern geomorphology and bathymetry (Figure 5).

Upper Rudeis Formation

The Upper Rudeis Formation at July field consists of deposits of a submarine-fan system that was sourced from the western rift shoulder and transported through the Morgan structural transfer zone. In areas of the Suez rift not near structural transfer zones, the Upper Rudeis Formation is predominantly fine grained, supporting the idea that structural transfer zones control the distribution of coarse-grained facies in rift basins (Lambiase and Bosworth, 1995).

The Upper Rudeis Formation contains two major sandstone units, the Hawara and Asl sandstones (Figure 2). The base of the Hawara sandstone occurs above the first downhole appearance of *Eggerella propinqua* (E.prop in Figure 2) and is sharp but generally not erosional (underlying units can be traced regionally). On wire-line logs, the Hawara sandstone is either massive or comprised of stacked, sharp-based units that show an overall upsection trend of increasing sonic and gamma-ray values, interpreted as fining and thinning-upward sequences (Figure 2). Sandstone is predominantly composed of quartz, with lesser amounts of feldspar and igneous, metamorphic or sedimentary rock fragments (Figure 6). The most likely source is the Red Sea Hills on the western rift shoulder, which consists of Precambrian igneous and metamorphic rocks, as well as a thick sequence of Cretaceous and older quartz-rich sandstone. Sedimentary facies observed in cores in

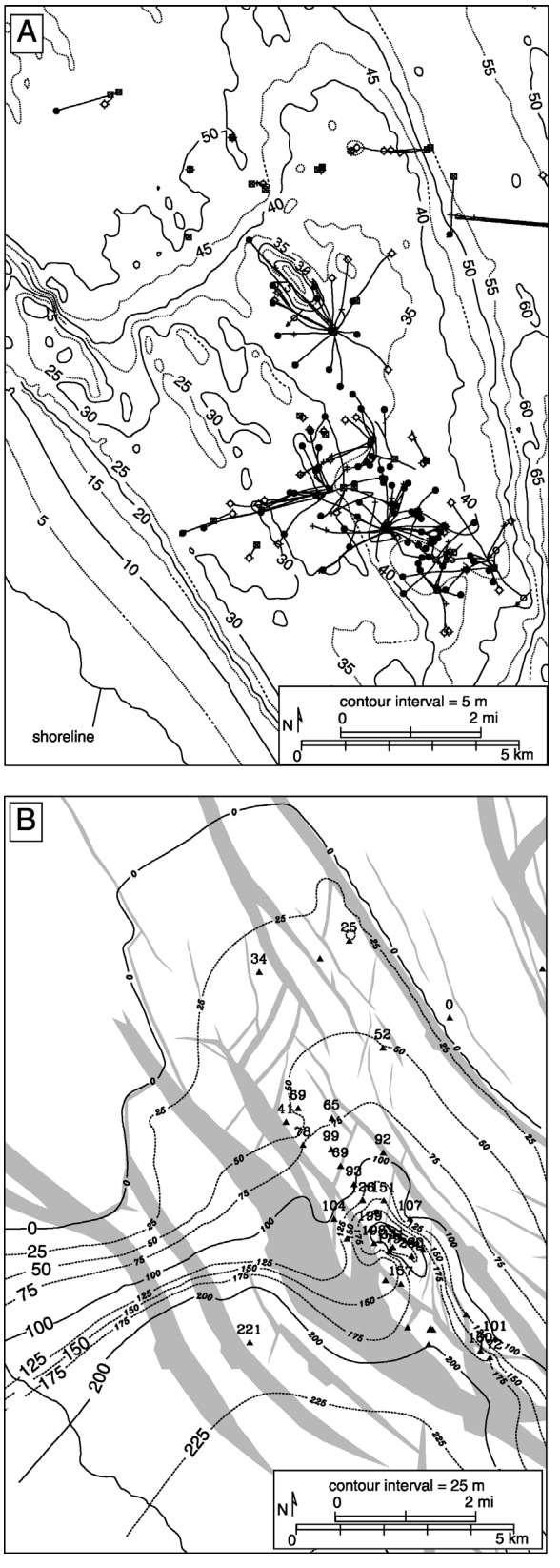

Figure 5. (A) Present-day bathymetry of the July field area, showing large delta system point sourced from the rift margin. (B) Net reservoir map of Lower Rudeis July sand (~19 m.y.) at July field. That and the modern bathymetry demonstrate the longevity of the depositional system in the July field area. Fault gaps in gray are at July sand level. See Figure 1B for location of map areas and Figure 2A for stratigraphic position of Lower Rudeis July sand.

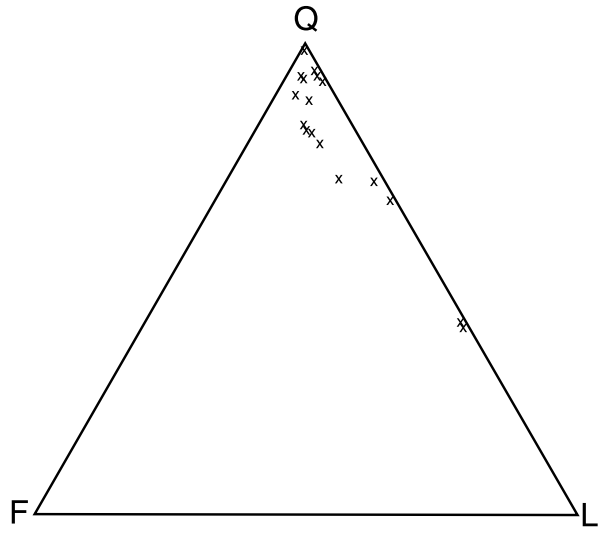

Figure 6. Ternary plot showing detrital composition of Hawara and Asl sandstones, based on point counts conducted on thin sections taken from whole core of the SG310-5A well. Q = quartz (monocrystalline and polycrystalline); F = all feldspars; L = sedimentary, igneous, and metamorphic lithic fragments and chert. See Figure 3 for the location of the well, Figure 7 for the location of thin sections in the core, and Figure 8A for the location of the core in the well.

the west July field area (Figure 7) include sharp-based, medium- to fine-grained sandstone (with rare pebble conglomerate) arranged as fining-upward sequences 1–6 m (~3–18 ft) thick, with rip-up clasts, cross-beds (commonly deformed), horizontal laminations, ripples, internal scour surfaces, burrows, shell fragments, and foraminiferal tests. Trace fossils and ichnofacies include *Planolites*, *Palaeophycus*, *Thalassinoides*, *Zoophycos*, *Helminthoidea*, and *Glossifungites* in shale directly below sharp-based sandstone units. The most common upsection facies transition includes cross-bedded or massive sandstone to laminated sandstone to laminated or ripple-marked siltstone or mudstone (Bouma sequences; Figure 7). Although water depth is difficult to determine, no shallow-water features (e.g., wave-generated ripples, mud-draped ripples, mud cracks) are present. The trace-fossil assemblages observed are not indicative of shallow-water deposition and are found in deep-water deposits (Bromley, 1990; Pemberton et al., 2002). The Hawara sandstone is overlain by dark shale containing calcite nodules and rare trace fossils (*Chondrites* and *Planolites*). Thus, we interpret the Hawara sandstone as consisting of turbidites, most likely deposited on a delta slope or submarine fan sourced from the western rift margin in water depths greater than the storm wave base. Correlation of wire-line logs and paleontological data with wells located to the west indicates that sediment was transported from the western rift shoulder to the July field area.

The top of the Asl sandstone occurs at a lithologic change from fine-grained calcareous mudstone to foraminiferal grainstone and sandstone, commonly near the first downhole appearance of the foraminiferal assemblage *Praeorbulina glomerosa curva* (P.curv in Figure 2). This corresponds to an abrupt shift in the sonic log. The log pattern for the Asl sandstone is similar to the Hawara sandstone, with sonic and gamma-ray values increasing upsection, interpreted as a fining- and thinning-upward trend (Figure 2). Sedimentary facies identified in core and detrital composition are similar to the Hawara sandstone (Figure 6), and we interpret the Asl to have been deposited as turbidites on a delta slope or submarine fan sourced from the west. However, unlike the Hawara sandstone, the Asl sandstone contains carbonate nodules, foraminiferal grainstone, black mudstone, and more evenly distributed burrows (Figure 7). This could indicate an environment located more distal on the submarine fan system than the underlying Hawara sandstone, or a decrease in the coarse sediment input to the basin. Trace-fossil abundance decreases near the top of the Asl sandstone.

Ayun Musa Formation

The Ayun Musa Formation is divided into the lower Lagia shale (including the Markha anhydrite) and upper Ras Budran Member (Figure 2). The base of the lower Lagia shale occurs above the Asl sandstone and is generally barren of fossils. Paleodepositional environments are difficult to interpret because of lack of faunal content, but the lack of fossils may record shallow and saline water, fresh water (Wescott et al, 2000), or deeper water in a restricted basin. The Markha anhydrite is about 3–15 m thick (~10–50 ft) (Figure 2) and is associated with algal mounds (Wescott et al., 1996). It is interpreted to have been deposited as a shallow-water sabkha. The top of the Lagia shale is defined by the top of a coarsening-upward sequence associated with the first downhole appearance of *P. glomerosa circularis* (P.glom in Figure 2). The top of the Ras Budran Member is defined by the base of the anhydrite of the Belayim Formation, and contains the first downhole appearances of foraminifera *Globorotalia peripheroronda* (Gr.per in Figure 2). In the July field area, facies are predominantly shaly, with small amounts of sandstone.

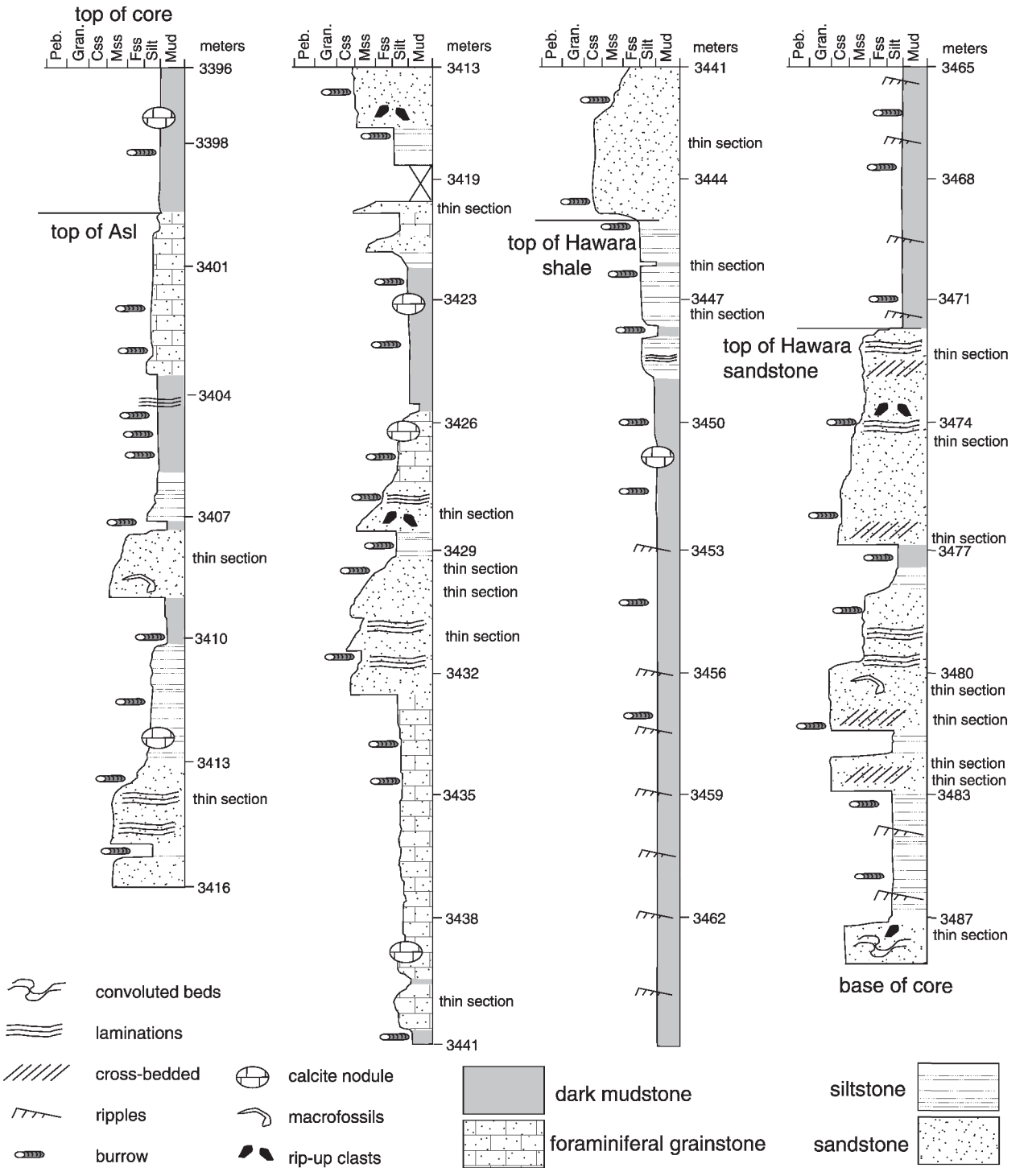

Figure 7. Log of core description from SG310-5A well in the west July field area. Depths are measured core depths. See Figure 8A for the position of the cored interval in the well and Figure 3 for location of the well.

Belayim Formation

The Belayim Formation consists of mixed anhydrite, salt, shale, sandstone, and limestone and records deposition in shallow-water environments. The first downhole appearance of foraminifera *Globigerinoides mitra* occurs in the upper member (Gs.mit in Figure 2). It is thin to absent on the crest of the July block and attains its maximum thickness in the immediate hanging wall of the July-B fault and the west July fault (Figure 4).

DISCUSSION

Controls on Synrift Sedimentation in the July Field Area

The July block did not grow as a single, large fault block, bounded by a single, large-displacement, normal fault. Instead, multiple fault blocks in the July field area controlled Miocene sediment thickness and depositional patterns. Gross interval and net reservoir thicknesses in the Asl and Hawara sandstones change abruptly across the west July fault and not the main July-B fault, indicating that the west July fault accommodated most of the deformation in the July field area at that time (Figures 8A, 9, 10). During Hawara deposition, several structural lows existed on the July block in the hanging walls of cross faults that were oriented oblique to the main rift-parallel trend (Figure 8B). Sandstone thickness is greater in these areas than in the rest of the block (Figures 9, 11A). Cross faults have been shown to control synrift sediment distribution elsewhere in the Suez rift (Allen et al., 1984; Bosworth et al., 1998; Winn et al., 2001).

The Asl sandstone records another episode of synrift, coarse clastic deposition in the July field area (Figure 10). Like the Hawara sandstone, the west July fault controlled stratal thickness, and the July-B fault appears to have been relatively inactive (Figure 8). The Asl does not appear to have been affected by cross faults in the July block, and thickness patterns do not mimic those of the older Hawara sandstone (Figures 8–11).

Abrupt changes in thickness across the west July fault indicate hundreds of feet of displacement during deposition of the Ayun Musa Formation (Figure 12A). Thickness trends cut across the July B fault, suggesting that it was not yet an active, throughgoing fault. Although there is no associated major influx of coarse sediment in the July field area during this period, thick accumulations of coarse-grained sediment of this age occur near other structural transfer zones in the Suez rift (e.g., El Morgan field; Figure 1).

The absence of the Belayim Formation on the crest of July field is caused by a combination of nondeposition during uplift of the block along the July-B fault and erosion (Figure 12b). Wells downdip from the crest have all members of the formation, and all members thin updip toward the crest. The west July fault tips out (loses displacement) in the upper part of the formation, indicating that motion on this fault ceased during Belayim deposition (Figure 4). The July-B fault cuts through the Belayim Formation and tips out below the top of the South Gharib Formation. We interpret that the west July fault transferred its displacement to the July-B fault during Belayim deposition, and that motion on the July-B fault continued throughout South Gharib deposition. This is when tilting of the July block occurred, creating a wedge of Belayim-aged sedimentary rocks on the footwall (Figure 4).

Synrift Depositional Models and Fault-Block Evolution

Synrift sediment thickness patterns in the July field area enable us to determine the timing of faulting and evolution of the July block. The July-B fault did not have major displacement and did not have a major effect on sediment thickness until after deposition of the Ayun Musa Formation. The fault that had the most control on Upper Rudeis and Ayun Musa deposition, the west July fault, appears to have ceased motion after deposition of the Belayim Formation. Thus, the July field area has an episodic growth history that involves multiple faults.

The Upper Rudeis through Belayim Formation isopach maps provide insight into how the July block evolved (Figures 9, 10, 12). Based on these maps (except the Belayim map, Figure 12b), thickness trends appear either to be unaffected by or to cut across the present-day July-B fault. What is presently the structural crest of the block was formerly a depositional sink. This records the presence of two or more independent normal-fault segments, expressed at the sea floor as fault-propagation folds, which later linked to form the July-B fault (Figure 13a). The regions between the fault segments were structural lows where sediment accumulated. These areas were later broken by cross faults that linked the rift-parallel fault segments. We interpret that the fault segments linked and propagated to the sea floor during late Ayun Musa and into Belayim deposition, accelerating the displacement rate of the July-B fault, while the west July fault ceased motion. At that time, the crest of the block, formerly a structural low where sediment thickness was greater than surrounding areas, became structurally high and the area of the least sediment accumulation (Figure 13b). Other models for sedimentation around unlinked fault segments that subsequently link have been presented by Gawthorpe et al. (1997) and Jackson et al. (2002).

This model has important implications for the prediction of coarse-grained synrift sedimentary rocks on and around normal-fault blocks. Commonly, deposits

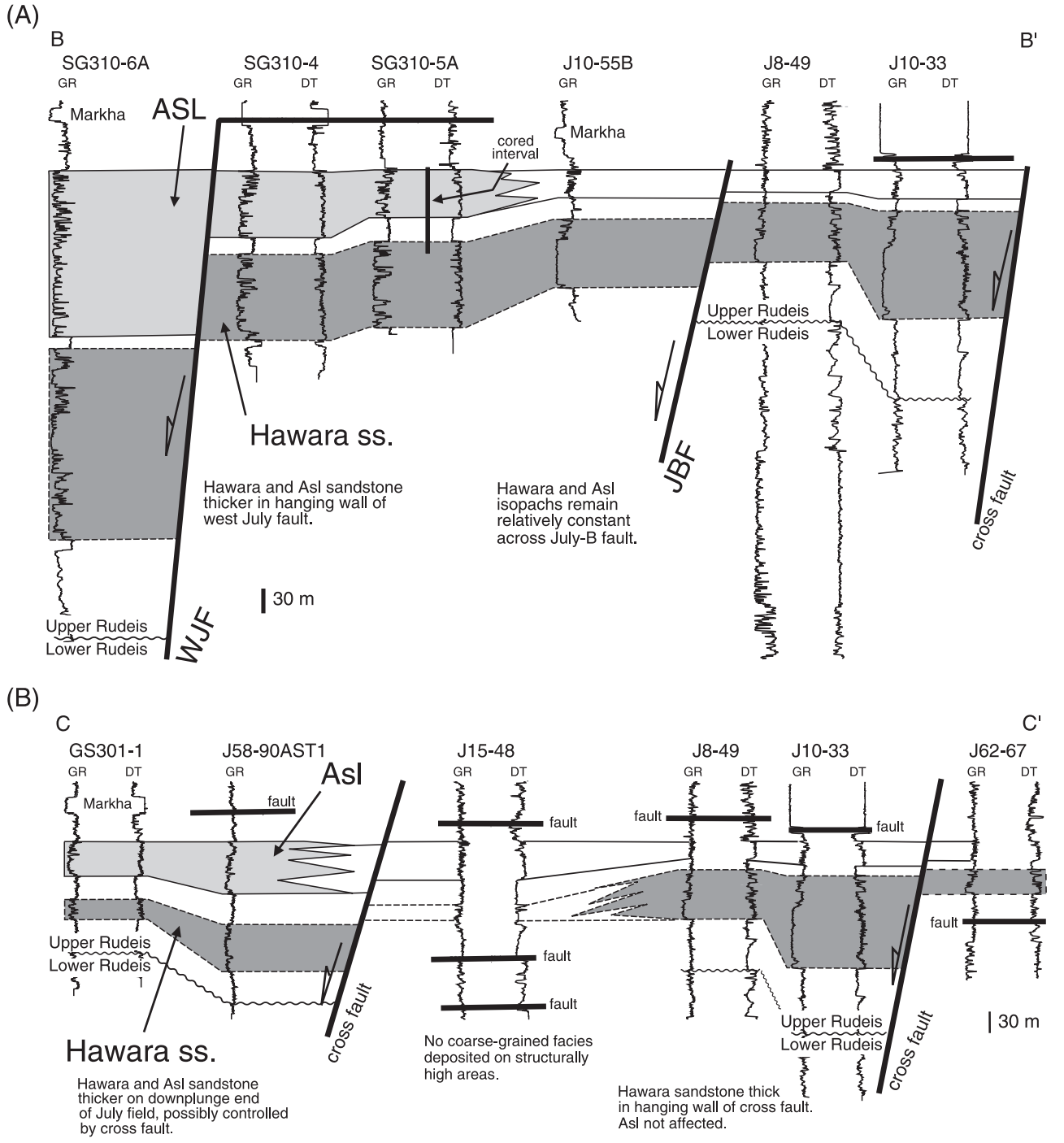

Figure 8. (A) Stratigraphic correlation panel for the Upper Rudeis Formation from west July field area to southeastern July field. The most dramatic thickness changes occur across the west July fault (WJF) and not the July-B fault (JBF), which presently bounds the field. (B) Stratigraphic correlation panel for the Upper Rudeis Formation from southern to northern July field. Thickness changes in Hawara sandstone occur across cross faults, and the Asl sandstone retains a relatively constant thickness. Both sections hung on the top of the Asl sandstone. See Figure 9 for location of lines. Logs are gamma ray (GR; 0–100° API) and sonic (DT; 140–40 ms).

of equivalent age are thought to thin toward the footwall crest and thicken into the hanging wall of major fault blocks (e.g., Proser, 1993; Ravnas and Steel, 1998), and indeed, this can be demonstrated elsewhere in the Suez rift (Dolson et al., 1996; Ramzy et al., 1996). Using this model, and without well control or

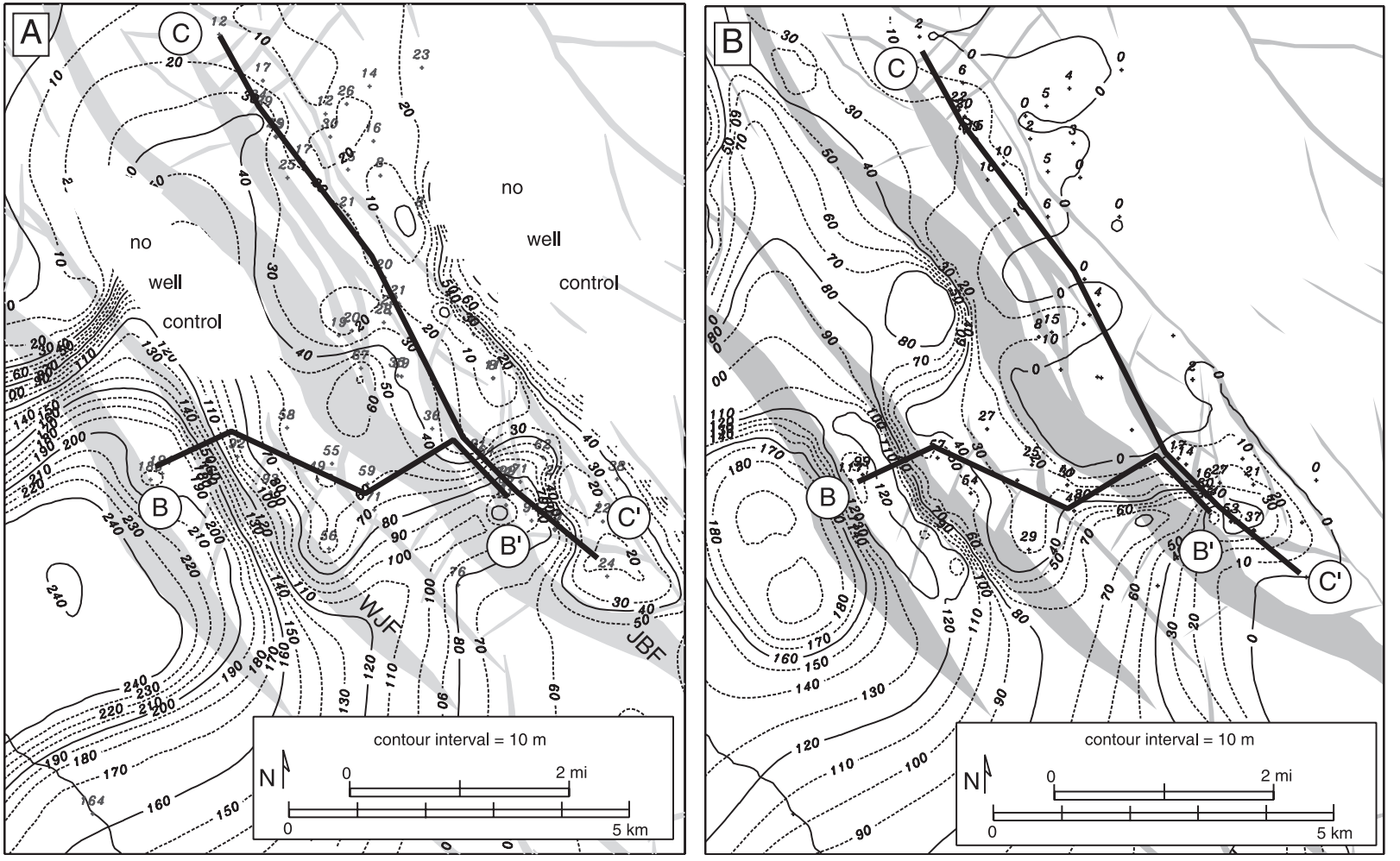

Figure 9. (A) Gross interval isopach map, Hawara sandstone, based on well control and 3-D seismic data. (B) Net reservoir isopach map, Hawara sandstone, based on well control. In both maps, note that dramatic thickness changes occur across the west July fault (WJF) and a cross fault located in the southern part of the field. The July-B fault (JBF), which presently bounds the July block, does not appear to have had significant influence on thickness or sand distribution. Effective porosity logs were calculated from neutron-density and gamma-ray logs, and a 10% cutoff was used to define reservoir-quality rock. Both maps show true stratigraphic thickness. Fault gaps in gray are at top Hawara sandstone. See Figure 1B for location of map areas. Lines of correlation BB′ and CC′ are shown in Figure 8.

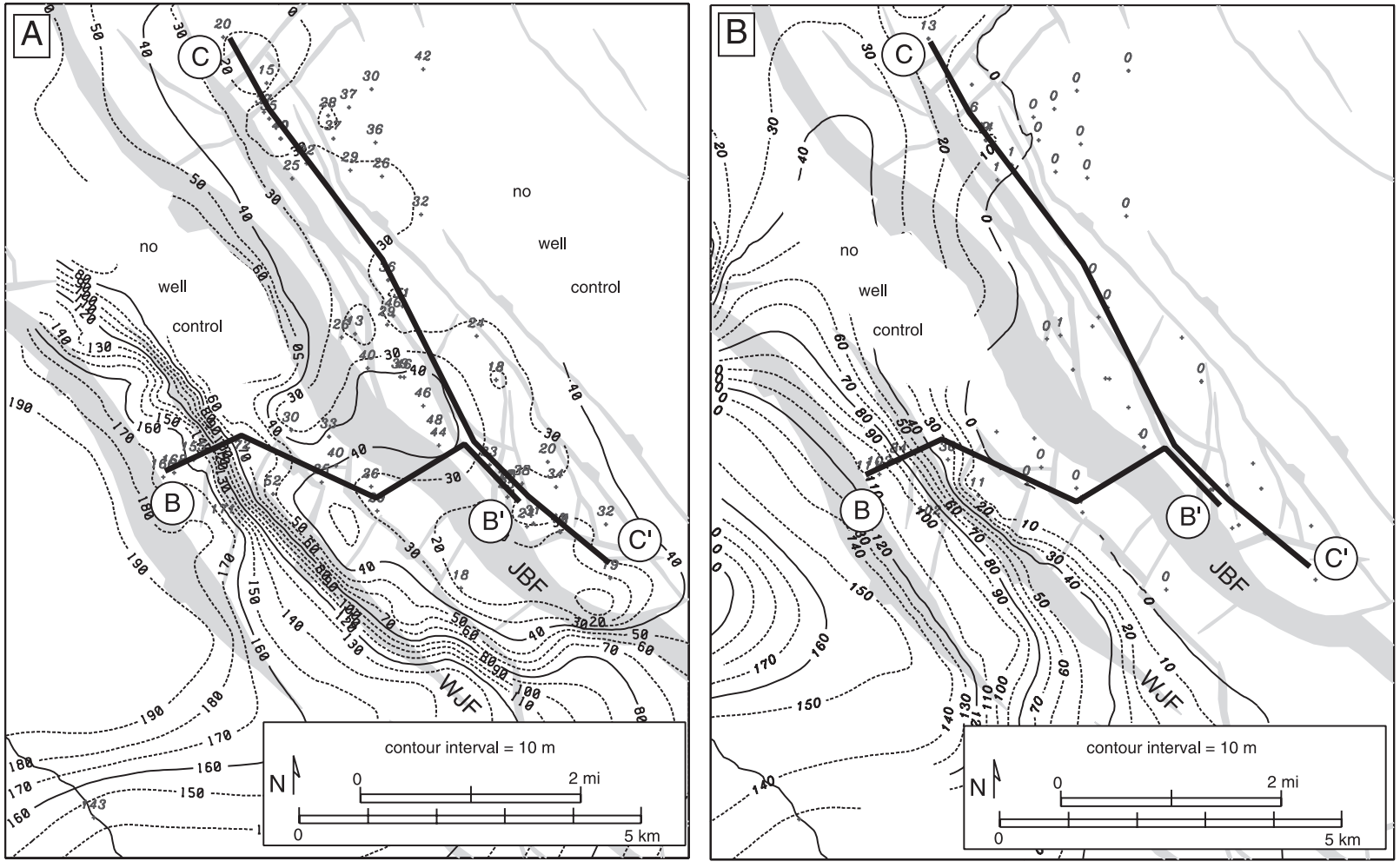

Figure 10. (A) Gross interval isopach map, Asl sandstone, based on well control and 3-D seismic data. (B) Net reservoir isopach map, Asl, based on well control. In both maps, thickness changes abruptly across the west July fault (WJF) and not the July-B fault (JBF), which presently bounds the July block. Effective porosity logs were calculated from neutron-density and gamma-ray logs, and a 10% cutoff was used to define reservoir-quality rock. Both maps show true stratigraphic thickness. Fault gaps in gray are at top of the Asl sandstone. See Figure 1B for location of map areas. Lines of correlation BB′ and CC′ are shown in Figure 8.

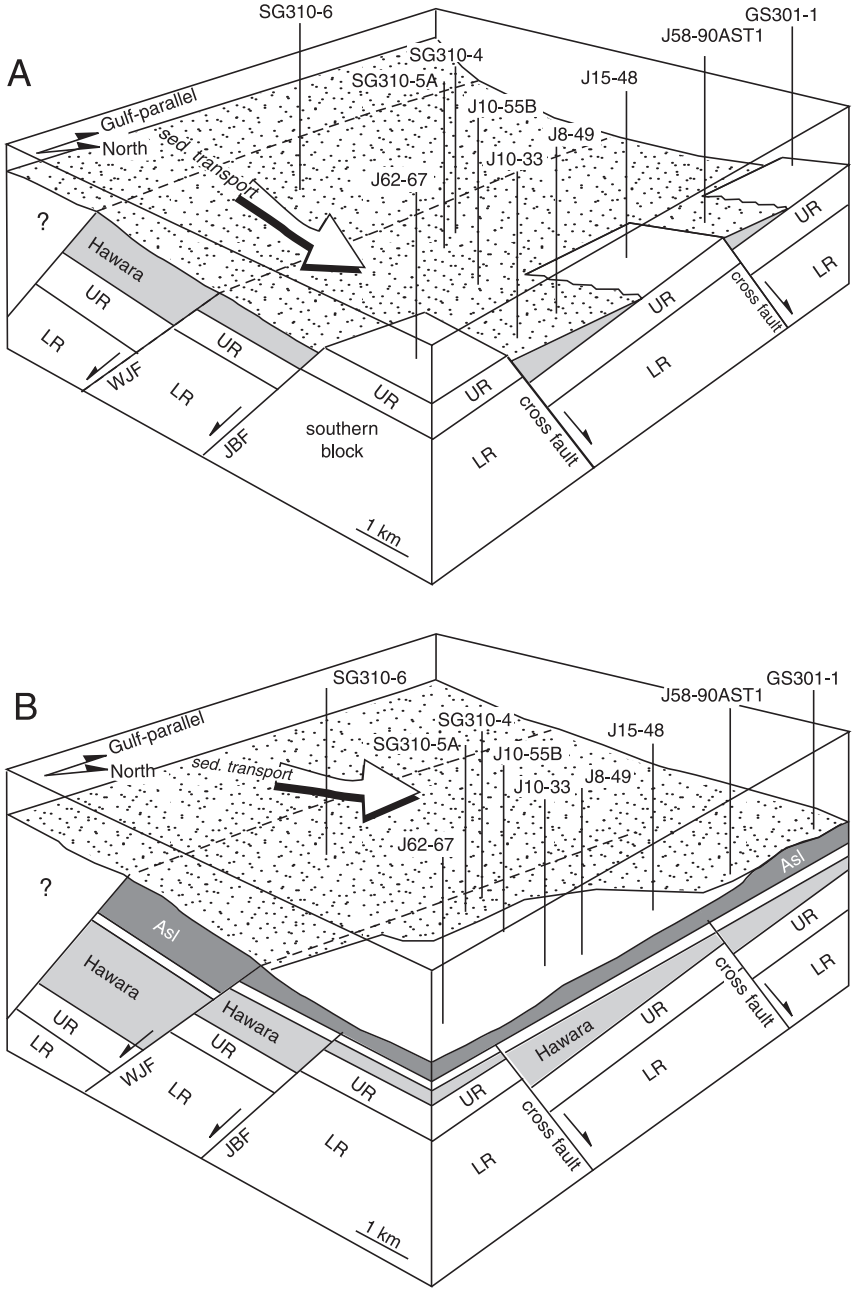

Figure 11. (A) Three-dimensional block diagram showing depositional model for Hawara sandstone. Sediment thickness changes most abruptly across west July fault (WJF). Sandstone facies extend across the July-B fault (JBF) and accumulated in structural lows adjacent to cross faults in July block. (B) Three-dimensional block diagram showing depositional model for Asl sandstone. Sediment thickness changes most abruptly across the west July fault. Wells correspond to wells shown in Figure 8. LR = Lower Rudeis Formation; UR = Upper Rudeis Formation.

high-quality seismic data, one might have chosen to explore for thick Upper Rudeis clastic rocks in the immediate hanging wall of the July-B fault (Well B, Figure 14) or for stratigraphic traps near the crest of the July block (Well A, Figure 14). However, the Upper Rudeis Formation does not thin onto the crest of the July block, nor does it consistently thicken in the immediate hanging wall of the July-B fault. Instead, the west July fault, west of the main field, in conjunction with cross faults in the main July block, controlled stratal thickness, and the July block was not a major syndepositional structural feature. Because of the poor quality of seismic data in the Gulf of Suez, the complexity of the evolution of the July block, involving laterally variable synrift thickness, linkage of independent fault segments, and transferring of displacement between the west July and July-B faults, would not be recognized without dense well control.

CONCLUSIONS

Thickness patterns and sedimentary facies in the Upper Rudeis Formation record the episodic growth of the

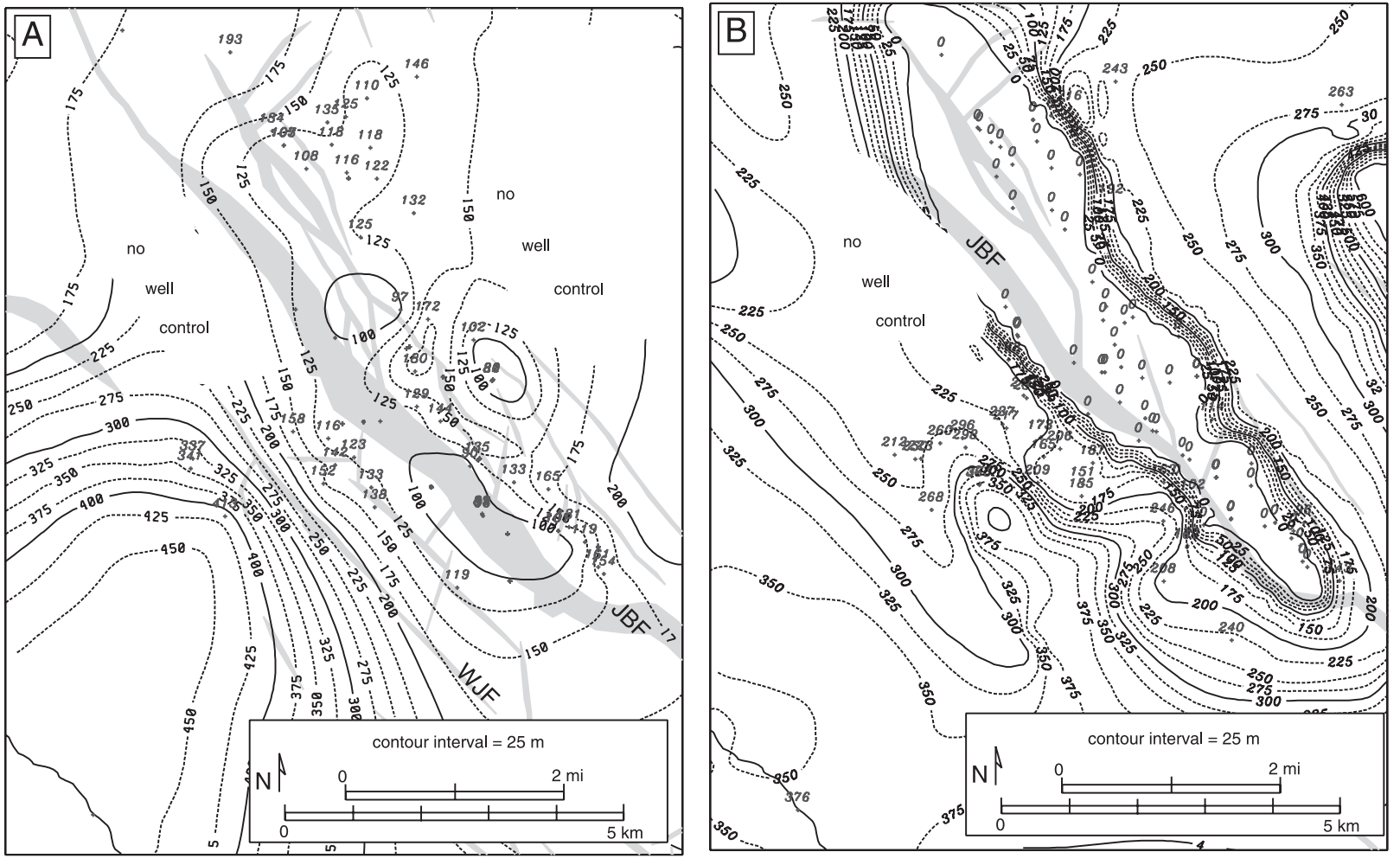

Figure 12. (A) Gross interval isopach map, Ayun Musa Formation, based on well control and 3-D seismic data. The west July fault (WJF) controlled stratal thickness, but isopach trends crosscut the July-B fault (JBF). Fault gaps in gray are at top Ayun Musa Formation. (B) Gross interval isochore map, Belayim Formation, based on well control and 3-D seismic data. During Belayim deposition, the July-B fault was the main control on thickness patterns, whereas displacement on the west July fault ceased. Fault gaps in gray are at top Belayim Formation. See Figure 1B for location of map areas.

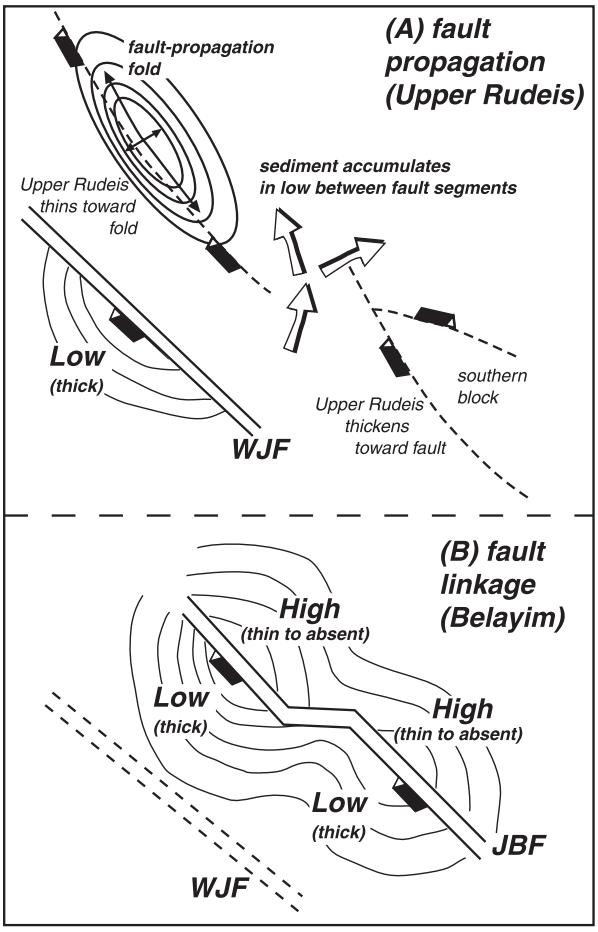

Figure 13. Evolution of July block. (A) During Upper Rudeis and lower Ayun Musa deposition, the west July fault (WJF) controlled thickness and sandstone distribution. The July-B fault (JBF) consisted of a series of small-displacement, unlinked fault segments, which also controlled depositional patterns. (B) During deposition of upper Ayun Musa and Belayim formations, displacement on the WJF ceased, and individual segments linked to form the JBF, a geometry reflected in the present structure.

July structural block. The present-day structural configuration is different from that during Upper Rudeis deposition. At that time, the major block-bounding fault, the July-B fault, was most likely a series of small-displacement, independent fault segments expressed at the sea floor as fault-propagation folds, and the major fault controlling synrift deposition was the west July fault. After deposition of the Ayun Musa Formation, deformation was transferred from the west July fault to the July-B fault, which was formed by the linkage of several fault segments.

Models of synrift sedimentation and their structural controls need to be developed with knowledge of paleostructural configurations. In a basin such as the

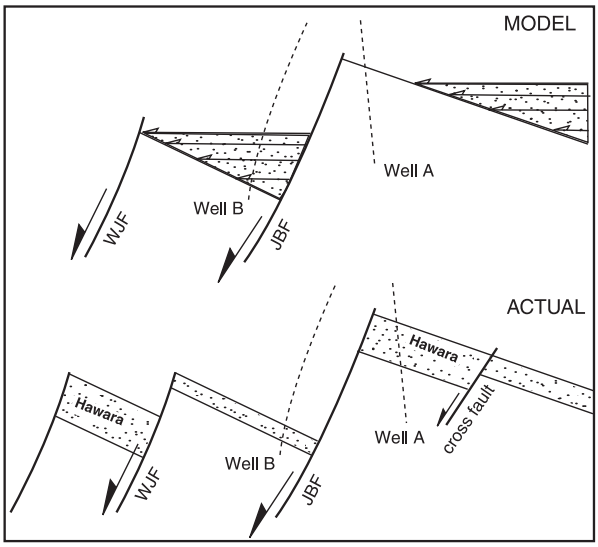

Figure 14. Generalized diagram showing model-driven prognosis for Upper Rudeis sandstone distribution (top) vs. actual sandstone distribution (bottom). WJF = west July fault; JBF = July-B fault.

Suez rift, where seismic data are of poor quality, complex evolution of structural blocks may not be detected without abundant well control.

REFERENCES CITED

Allen, G., A. Ayyad, G. Desforges, M. Haddadi, and J. Pizon, 1984, Subsurface sedimentological study of the Rudeis Formation in Kareem, Ayun, Yusr and Shukheir fields, *in* Proceedings of the 6th Exploration Conference: Cairo, Egyptian General Petroleum Corporation, p. 164–176.

Bosence, D. W. J., 1998, Stratigraphic and sedimentological models of rift basins, *in* B. H. Purser and D. W. J. Bosence, eds., Sedimentation and tectonics in rift basins, Red Sea— Gulf of Aqaba: London, Chapman & Hall, p. 9–25.

Bosworth, W., and K. McClay, 2001, Structural and stratigraphic evolution of the Gulf of Suez rift, Egypt: a synthesis, *in* P. A. Zeigler, W. Cavazza, A. H. F. Robertson, and S. Crasquin-Soleau, eds., Peri-Tethyan rift-wrench basins and passive margins: Paris, Musee Nationale d'Histoire Naturelle, p. 567–606.

Bosworth, W., P. Crevello, R. D. Winn Jr., and J. Steinmetz, 1998, Structure, sedimentation, and basin dynamics during rifting of the Gulf of Suez and north-western Red Sea, *in* B. H. Purser and D. W. J. Bosence, eds., Sedimentation and tectonics in rift basins, Red Sea–Gulf of Aqaba: London, Chapman & Hall, p. 77–96.

Bromley, R. G., 1990, Trace fossils: London, Unwin Hyman, 280 p.

Dolson, J., O. El-Gendi, H. Charmy, M. Fathalla, and I. Gaafar, 1996, Gulf of Suez rift basin sequence models. Part A, Miocene sequence stratigraphy and exploration significance in the Greater October field area, *in* Proceedings of the 16th Exploration Conference: Cairo, Egyptian General Petroleum Corporation, p. 1–8.

El Heiny, I., and N. Enani, 1990, Miocene conglomerate beds in

Rudeis and Belayim oil fields and their surface analogues, *in* Proceedings of the 10th Exploration Conference: Cairo, Egyptian General Petroleum Corporation, p. 431–457.

Garfunkel, Z., and Y. Bartov, 1977, The tectonics of the Suez rift: Geological Survey of Israel Bulletin 71, 44 p.

Gawthorpe, R. L., and J. M. Hurst, 1993, Transfer zones in extensional basins: their structural style and influence on drainage development and stratigraphy: Journal of the Geological Society (London), v. 150, p. 1137–1152.

Gawthorpe, R. L., A. Fraser, and R. E. Collier, 1994, Sequence stratigraphy in active extensional basins: implications for the interpretation of ancient basin-fills: Marine and Petroleum Geology, v. 11, p. 642–658.

Gawthorpe, R. L., I. R. Sharp, J. R. Underhill, and S. Gupta, 1997, Linked sequence stratigraphic and structural evolution of propagating normal faults: Geology, v. 25, p. 795–798.

Gupta, S., J. R. Underhill, I. R. Sharp, and R. L. Gawthorpe, 1999, Role of fault interactions in controlling synrift sediment dispersal patterns: Miocene, Abu Alaqa Group, Suez rift, Sinai, Egypt: Basin Research, v. 11, p. 167–189.

Hosny, W., I. Gafaar, and A. Sabour, 1986, Miocene stratigraphic nomenclature in the Gulf of Suez region, *in* Proceedings of the 8th Exploration Conference: Cairo, Egyptian General Petroleum Corporation, p. 131–148.

Jackson, C. A. L., R. L. Gawthorpe, and I. R. Sharp, 2002, Growth and linkage of the east Tanka fault zone, Suez rift: structural style and synrift stratigraphic response: Journal of the Geological Society (London), v. 159, p. 175–187.

Krebs, W. N., W. A. Wescott, D. Nummedal, I. Gaafar, G. Azazi, and S. A. Karamat, 1997, Graphic correlation and sequence stratigraphy of Neogene rocks in the Gulf of Suez: Bulletin de la Societe Geologique de France, v. 168, p. 63–71.

Lambiase, J. J., and W. Bosworth, 1995, Structural controls on sedimentation in continental rifts, *in* J. J. Lambiase, ed., Hydrocarbon habitat in rift basins: London, Geological Society of London, p. 117–144.

Matbouly, S., and M. El Sabbagh, eds., 1996, Gulf of Suez oil fields, a comprehensive overview: Cairo, Egyptian General Petroleum Corporation, 736 p.

McClay, K. R., G. J. Nichols, S. M. Khalil, M. Darwish, and W. Bosworth, 1998, Extensional tectonics and sedimentation, eastern Gulf of Suez, Egypt, *in* B. H. Purser and D. W. J. Bosence, eds., Sedimentation and tectonics in rift basins, Red Sea–Gulf of Aqaba: London, Chapman & Hall, p. 211–238.

Morley, C. K., R. A. Nelson, T. L. Patton, and S. G. Munn, 1990, Transfer zones in the east African rift system and their relevance to hydrocarbon exploration in rifts: AAPG Bulletin, v. 74, p. 1234–1253.

Moustafa, A. M., 1976, Block faulting in the Gulf of Suez, *in* Abstracts of papers presented at the 5th Exploration Seminar: Cairo, Egyptian General Petroleum Corporation, p. 19.

Moustafa, A. R., 1995, Internal structure and deformation of an accommodation zone in the northern part of the Suez rift: Journal of Structural Geology, v. 18, p. 93–107.

Moustafa, A. R., 2002, Controls on the geometry of transfer zones in the Suez rift and northwest Red Sea: implications for the structural geometry of rift systems: AAPG Bulletin, v. 86, p. 979–1002.

National Stratigraphic Sub-Committee of the Geological Sciences of Egypt, 1974, Miocene rock stratigraphy of Egypt: Egyptian Journal of Geology, v. 18, p. 1–69.

Nelson, R. A., T. L. Patton, and C. K. Morely, 1992, Rift-segment interaction and its relation to hydrocarbon exploration in continental rift systems: AAPG Bulletin, v. 76, p. 1153–1169.

Patton, T. L., A. R. Moustafa, R. A. Nelson, and S. A. Abdine, 1994, Tectonic evolution and structural setting of the Suez rift, *in* S. M. Landon, ed., Interior rift basins: AAPG Memoir 59, p. 9–55.

Pemberton, G., M. Spila, A. Pulham, T. Saunders, J. A. MacEachern, D. Robbins, and I. K. Sinclair, 2002, Ichnology and sedimentology of shallow to marginal marine systems: Ben Nevis & Avalon Reservoirs, Jeanne d'Arc Basin: Geological Association of Canada, Short Course Notes 15, 343 p.

Proser, S., 1993, Rift-related linked depositional systems and their seismic expression, *in* G. D. Williams and A. Dobb, Tectonics and seismic sequence stratigraphy: London, Geological Society of London, p. 35–66.

Ramzy, M., B. L. Steer, F. Abu-Shadi, M. Schlorholtz, and J. Mika, 1996, Gulf of Suez rift basin models. Part B, Miocene sequence stratigraphy and exploration significance in the central and southern Gulf of Suez, *in* Proceedings of the 16th Exploration Conference: Cairo, Egyptian General Petroleum Corporation, p. 1–7.

Ravnas, R., and R. J. Steel, 1998, Architecture of marine rift-basin successions: AAPG Bulletin, v. 82, p. 110–146.

Rhine, J. M., A. B. Hassouba, L. Shishkevich, A. Shafi, G. Azzazi, H. Nashaat, A. Badawy, and A. El Sisi, 1988, Evolution of a Miocene fan delta: a giant oil field in the Gulf of Suez, Egypt, *in* W. Nemec and R. J. Steel, eds., Fan deltas: sedimentology and tectonic settings: London, Blackie and Sons, p. 239–250.

Schutz, K. I., 1994, Structure and stratigraphy of the Gulf of Suez, Egypt, *in* S. M. Landon, ed., Interior rift basins: AAPG Memoir 59, p. 57–96.

Wescott, W. A., D. Nummedal, W. N. Krebs, and S. A. Karamat, 1996, Depositional facies of the early synrift strata on the Sinai margin of the Gulf of Suez, *in* Proceedings of the 13th Petroleum Conference: Cairo, Egyptian General Petroleum Corporation, p. 297–312.

Wescott, W. A., W. N. Krebs, P. A. Bentham, and D. T. Pocknall, 2000, Miocene brackish water and lacustrine deposition in the Suez rift, Sinai, Egypt: Palaios, v. 15, p. 65–72.

Winn Jr., R. D., P. D. Crevello, and W. Bosworth, 2001, Lower Miocene Nukhul Formation, Gebel el Zeit, Egypt: Model for structural control on early synrift strata and reservoirs, Gulf of Suez: AAPG Bulletin, v. 85, p. 1871–1890.

Younes, A. I., and K. R. McClay, 2002, Development of accommodation zones in the Gulf of Suez–Red Sea rift, Egypt: AAPG Bulletin, v. 86, p. 1003–1026.

Young, M. J., R. L. Gawthorpe, and I. R. Sharp, 2000, Sedimentology and sequence stratigraphy of a transfer zone coarse-grained delta, Miocene Suez rift, Egypt: Sedimentology, v. 47, p. 1081–1104.